K.R.V. (Raghu) Manikantachari
Center for Advanced Turbomachinery and Energy Research (CATER),
University of Central Florida,
Orlando, FL 32816
e-mail: raghu@ucf.edu

Ramees K. Rahman
Center for Advanced Turbomachinery and Energy Research,
University of Central Florida,
Orlando, FL 32816
e-mail: rameeskr@knights.ucf.edu

Scott M. Martin
Eagle Flight Research Center,
Embry-Riddle Aeronautical University,
Daytona Beach, FL 32114
e-mail: martis38@erau.edu

Carlos Velez
GE Global Research Center,
Niskayuna, NY 12309
e-mail: carlos.velez@ge.com

Subith S. Vasu
Center for Advanced Turbomachinery and Energy Research,
University of Central Florida,
Orlando, FL 32816
e-mail: subith@ucf.edu

Influence of Equation-of-States on Supercritical CO_2 Combustion Mixtures

Fossil fuel based direct-fired supercritical CO2 (sCO_2) cycles are gaining the attention of industry, academia, and government due to their remarkable efficiency and carbon capture at high-source temperatures. Modeling plays an important role in the development of sCO_2 combustors because experiments are very expensive at the designed operating conditions of these direct-fired cycles. Inaccurate density estimates are detrimental to the simulation output. Hence, this work focuses on comprehensive evaluation of the influence and applicability of various equation-of-states (EOS) which are being used in the supercritical combustion modeling literature. A state-of-the-art supercritical combustion modeling methodology is used to simulate counter-flow supercritical CO_2 flames by using various equation-of-states. The results show that using the corresponding state principle to evaluate compressibility factor is not accurate. Also, van der Waal type EOSs predictions can be as accurate as complex Benedict–Webb–Rubin EOSs; hence van der Waal EOSs are more suitable to simulate sCO_2 combustor simulations. Non-ideal effects are significant under the operating conditions considered in this work. The choice of EOS significantly influences the flame structure and heat release rate. Also, assuming the binary interaction parameter as zero is reasonable in sCO_2 combustion simulations. [DOI: 10.1115/1.4048666]

Keywords: supercritical CO_2 combustion, equation-of-state

1 Introduction

Studies have shown that supercritical CO_2 (sCO_2) power cycles have a potential to attain significantly higher efficiencies than conventional steam Rankine cycles [1,2] due to the attractive characteristics of sCO_2 just above its critical point. Near the critical zone, thermophysical properties such as density, specific heat, and viscosity of the fluid change significantly and sCO_2 cycles takes advantage of these changes to add additional points on the efficiency scale [1]. CSBOLDSTART CSBOLDENDIndustry, academia, and government are actively investing funds in developing solar, nuclear, geothermal, and fossil fuel based sCO_2 cycles. This work focuses on the modeling part of direct-fired, fossil fuel based sCO_2 cycles [3]. The extensive availability of natural gas over the globe is one important positive driving force for the direct-fired sCO_2 technology. Also, in this cycle, CO_2 can be captured completely without any additional cost for compression. It is estimated that a 300 MW direct-fired sCO_2 plant could produce one million gallons of the water per day [4]. Therefore, direct-fired sCO_2 cycles are standing as an attractive alternative for current high-source temperature, high-power cycles.

The direct-fired sCO_2 cycles work on a semi-closed cycle and uses sCO_2 as the working fluid, therefore, CO_2 produced by the direct-fired, oxy-methane combustion can be recirculated within the same cycle loop and the excess sCO_2 from the cycle can be used for other commercial purposes [3]. The current state-of-the-art, optimized sCO_2 combustor operating conditions are 200–300 atm pressure, 800–1000 K inlet temperature, and the percentage of sCO_2 should be more than 95% by mass. These unconventional and challenging operating conditions entail researchers to depend largely upon simulation methods during all phases of combustion chamber design and development. An accurate model must account validated kinetics, real gas thermal and transport properties through the equation-of-state, and high-fidelity turbulent combustion models. Ongoing direct-fired sCO_2 combustion research on validating the sCO_2 chemical kinetics [5–17], flame and thermal property measurements and modeling [18–22], cycle and component analysis [17,22–28] are available in the literature, however a detailed influence of equation-of-state (EOS) on sCO_2 flames is not available.

The EOS is a crucial model for density estimation in a simulation. As discussed earlier, the operating pressure of sCO_2 combustors is ~300 atm, which is the supercritical condition for many of the combustion reactants and products. At these pressures, the average mean free path between the mixture molecules is small and intermolecular forces are not negligible. Hence, the ideal gas assumption is not valid. The inaccuracies associated with the use of the ideal gas assumptions (IGA) for various components of the supercritical description were systematically assessed [29] and reported that, for hydrogen/air flames, the laminar flame speeds at high pressures were found to increase with the use of the non-ideal EoS. The counter-flow diffusion flames of oxygen and n-alkanes (CH_4-$C_{16}H_{34}$) over the entire thermodynamic fluid regime and a wide range of flow strain rates are studied by Wang et al. [30] and the relationship between heat release rate and the pressure was established. A theoretical framework is established to study the effect of flow strain rate on counter-flow diffusion flames for general fluids over the entire thermodynamic regime [31]. However, no comprehensive work is available in the literature

Contributed by the Advanced Energy Systems Division of ASME for publication in the Journal of Energy Resources Technology. Manuscript received July 24, 2020; final manuscript received August 7, 2020; published online October 27, 2020. Editor: Hameed Metghalchi.

which helps researchers to understand the influence of non-ideal effects and consequences of using a wrong model in sCO_2 combustion simulations. Therefore, an attempt is made in this work to study various real gas EOS models and their effect on sCO_2 combustion.

EOS models can be broadly classified into three types, they are, molecular-based, virial-type, and van der Waal type EOS [32,33]. Molecular-based approaches are very accurate but cannot be used in combustion simulations due to their complexity and demand of computational time. Virial type EOS such as Benedict–Webb–Rubin (BWR) EOS are less complex in their formulations compared to the molecular-based EOS, however still computationally very expensive [34]. The van der Waal (or cubic) type EOSs are easier to implement and are computationally faster. These EOSs were originally developed and validated for petroleum mixtures. Hence, care is needed in using them for combustion applications. Three early EOSs which were developed in this category are the Peng–Robinson (PEN), Redlich–Kwong (RED), and Soave–Redlich–Kwong (SOV) EOSs. A short review of van der Waals type EOS is reproduced from Ref. [19] and presented below to help the readers understand various parameters in the model.

The work of Patel [35] proposed a common cubic equation form for RED, SRK, and PEN EOSs as shown in Eq. (1)

$$Z^3 - (1 + B^* - uB^*)Z^2 + (A^* + wB^{*2} - uB^* - uB^{*2}) Z - A^*B^* - wB^{*2} - wB^{*3} = 0 \tag{1}$$

In Eq. (1), the term A^* is the non-dimensional attraction term and is equal to $a_m P/R^2T^2$ and B^* is the non-dimensional repulsive term and is equal to $b_m P/RT$. The mixing rules in Eqs. (2) and (3) are used to find a_m and b_m

$$a_m = \sum_{i=1}^{KK}\sum_{j=1}^{KK} X_i X_j (a_i a_j)^{1/2} - (1 - \overline{k_{ij}}) \tag{2}$$

and

$$b_m = \sum_{i=1}^{KK} X_i b_i \tag{3}$$

(define P, T, R, z, KK). Here, the subscript i refers to a species index, X_i represent mole fractions, a_i and b_i are attraction and repulsion properties of pure species as shown in Table 1, and k_{ij} are binary-interaction coefficients that are determined empirically.

The SOV is a modified version of RED. The RED is only dependent on the critical temperature (T_c) and critical pressure (P_c). While SOV and PEN additionally depend on the acentric factor (ω), which is a measure of non-sphericity, to improve the accuracy. Since these EOSs are empirical, using them in a simulation requires validation. Based on the application and available experimental data, many developments and modifications to these EOSs have been made to improve the accuracy. But it should be noted that there is no data available in the literature to validate these models for sCO_2 combustion.

Table 1 Coefficients for the cubic equation-of-state

EOS	u	w	b	a
RED	1	0	$\frac{0.08664RT_c}{8P_c}$	$\frac{0.42748}{64}\frac{R^2T_c^{2.5}}{P_cT^{0.5}}$
SOV	1	0	$\frac{0.08664RT_c}{8P_c}$	$\frac{0.42748}{64}\frac{R^2T_c^{2.5}}{P_cT^{0.5}}\,l$
PEN	2	−1	$\frac{0.07780RT_c}{8P_c}$	$\frac{0.42748}{64}\frac{R^2T_c^{2.5}}{P_cT^{0.5}}\,l$

Note: T_c: critical temperature of the species, P_c: critical pressure of the species, ω: acentric factor of the species, $l = [1 + f_\omega(1 - T_r^{0.5})]^2$. For SOV EOS, $f_\omega = 0.48 + 1.574\omega - 0.176\omega^2$ and for PRS EOS, $f_\omega = 0.37464 + 1.54226\omega - 0.26992\omega^2$.

2 Modeling

A counter-flow diffusion flame is simulated by a state-of-the-art methodologies and it is described in detail in the works of Refs. [17,19,22]. The implementation of real gas models in the counter-flow flame simulation is shown pictorially in Fig. 1. Here, real gas thermal conductivity and viscosity are modeled similar to our previous work [19]. Thermal conductivity is modeled with the Stiel and Thodos model [36,37] and viscosity is modeled with the Lucas model [37,38]. The UCF 1.1 chemical kinetic mechanism, which is derived from the Aramco 2.0 and updated with the rates from molecular dynamic simulations which are specifically calculated for sCO_2 combustion [5–7,39], are used. The performance of this mechanism at stoichiometric conditions is like those of Aramco 2.0. However, at lean condition the predictions are improved because of newly included rates which are specifically calculated for sCO_2 combustion. CHEMKIN-Real gas [40] is coupled with an OPPDIF code (a counter-flow flame solver) [41].

Counter-flow diffusion flames are significant in the field of non-premixed turbulent systems because the turbulent flame can be assumed as a combination of small laminar flamelets locally, therefore, the local strain effect on a turbulent flame can be studied simply by changing the strain (by changing the inlet boundary conditions) of the counter-flow diffusion flame. Studies on these flames are very useful for understanding physics involved in combustion because unlike other simple reactor models, these flames include diffusion. A schematic of a counter-flow diffusion flame is shown in Fig. 2. Here, the fuel jet consists of pure methane at 300 K and the oxidizer jet consists of a O_2 and CO_2 mixture at 1000 K. In an actual combustor we can expect a wide range of CO_2 percentage in the combustion chamber and it is not possible to simulate all those possibilities in a counter-flow flame. Hence, only two compositions of CO_2 in the oxidizer stream are tested here. Tested conditions are shown in Table 2. Each simulation is performed with real gas and IGA for comparison.

A recent conceptual sCO_2 combustor model [21] has the inlet fuel jet at ~300 K and oxidizer jet at 1000 K temperature. The same fuel and oxidizer inlet conditions are used in this work. The mixture averaged diffusion and Dufour effects are accounted for in the modeling. Simulations are carried out at 300 atm. pressure.

3 Results and Discussion

3.1 State of sCO_2 Combustion. As the reactants transform into products, the critical state of the system also changes. In a typical rocket combustor (LH_2-LO_2 system), which generally operates at 100 atm., the products of combustion will be at a subcritical pressure though the reactants are supercritical because the critical point of H_2O is ~220 atm. Gradients of thermal properties are

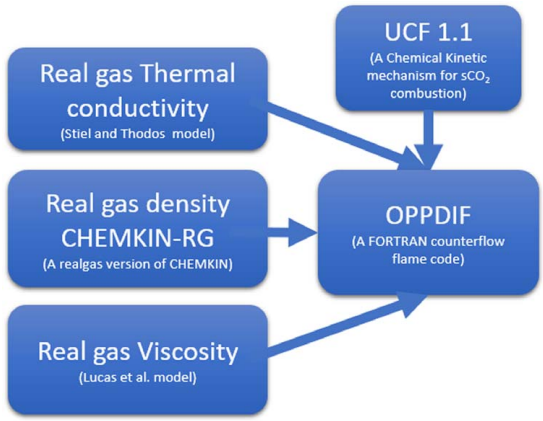

Fig. 1 A pictorial representation of the state-of-the-art real gas modeling implementation in the current study

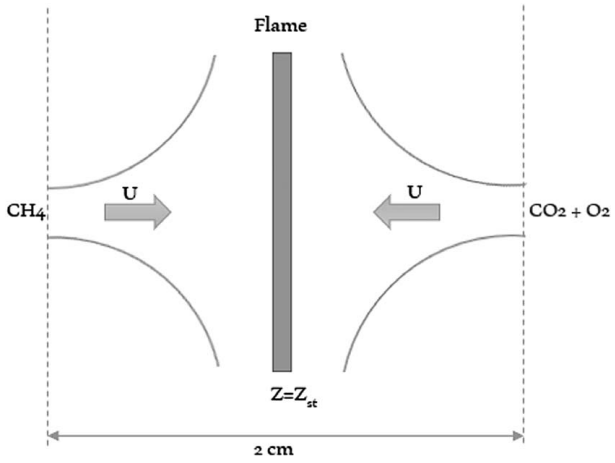

Fig. 2 A schematic diagram of the counter-flow diffusion flame (U is the inlet velocity boundary condition and Z_{st} is the stoichiometric mixture fraction)

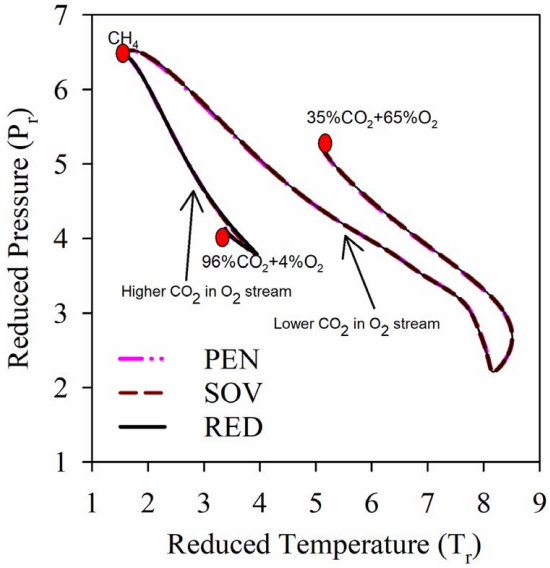

Fig. 3 Variation of T_r and P_r in counter-flow sCO_2 flame when higher and lower CO_2 are present in the oxidizer stream

larger when the reduced pressure (P_r) and reduced temperature (T_r) are close to unity and smaller when P_r and T_r are far from unity. Hence, it will be instructive to look at various P_r and T_r and how they are influenced by the choice of EOS. Here, critical properties of the combustion mixture between two jets are estimated by Eqs. (4) and (5) and divided by the solution temperature and pressure at corresponding points to obtain the reduced properties (give reference). Also, PEN, SOV, and RED EOSs are compared.

Critical temperature of the mixture T_{cm}:

$$T_{cm} = \sum_i x_i T_{ci} \tag{4}$$

Here, T_{ci} is the critical temperature of the individual species.

Critical pressure of the mixture P_{cm}:

$$P_{cm} = \sum_i x_i P_{ci} \tag{5}$$

Here, P_{ci} is the critical pressure of the individual species.

Figure 3 shows the variation of P_r and T_r in a counter-flow sCO_2 flame when higher and lower CO_2 are present in the oxidizer stream as described in Table 2. For both the cases, only CH_4 is present in the fuel jet, hence two curves originate from the top left point in the figure and depending upon the percentage of CO_2 present in the oxidizer stream, the curve bifurcates. The result shows that the combustion mixture obtains a minimum P_r when there is less CO_2 in the oxidizer side due to the presence of more H_2O in the products of the system. Also, the reactants and products are in supercritical state at both pressure and temperature. Further, the choice of EOS does not influence the range and the profile of reduced properties in the combustion. But further results show EOS influences kinetics and the fluid mechanic phenomenon in sCO_2 combustion.

3.2 Adoptability of Virial and van der Waal Type Equation-of-States. As discussed in the introduction, EOSs based on molecular dynamic approach are not suitable for combustion simulations; hence, the effect and applicability of the remaining two types of EOSs, i.e., virial and van der Waal type EOSs are discussed next.

3.2.1 Virial Type Equation-of-States. The BWR EOS is the most used virial type EOS in the supercritical combustion simulation due to its accuracy [34]. The superior performance of this EOS for pure substances over conventional van der Waals type EOS is well proven. The constants involved in this EOS formulation are only available for few pure substances. However, the works of Refs. [34,42] use this EOS in combination with the extended corresponding-state (ECS) principle. In this methodology, the combustion mixture is assumed as a pseudopure substance and its properties are evaluated by the well-known corresponding-state principle. In this way, BWR constants of known pure fluid are enough to evaluate the properties of combustion mixtures. A detailed description of using BWR along with the corresponding state principle for supercritical combustion simulation can be found in the work [34]. The corresponding-state principle states that all fluids at the same reduced temperature and pressures have the same compressibility factor (z) [43]. Factually, there will be a slight difference between one fluid and another, but the overall trend of z variation is the same with respect to reduced properties. The generalized compressibility factor graphs may have considerable errors for strongly polar gases (gases for which the centers of positive and negative charge do not coincide). In such cases the estimate for z may be in error by as much as 15–20%. The quantum gases hydrogen, helium, and neon do not conform to the corresponding-states behavior. Moreover, no literature confirms the corresponding state behavior of mixtures that are encountered in combustion. Further, at supercritical conditions, one should be cautious to use corresponding state principle because it is not proven that the fluids follow this behavior at P_r and T_r which are encountered in combustion. Also, it is known that the polarity and the interaction between molecules are also needed to be accounted for accurate density predictions.

Table 2 Tested conditions in the counter-flow simulation

Case	Description	Y_{CH_4} in the fuel jet	Fuel jet temperature	Y_{CO_2} in oxidizer jet	Oxidizer jet temperature	Pressure	EOSs
1	Higher CO_2	1	300 K	0.96	1000 K	300 atm.	IGA, PEN, RED, SOV
2	Lower CO_2	1	300 K	0.35	1000 K	300 atm.	IGA, PEN, RED, SOV

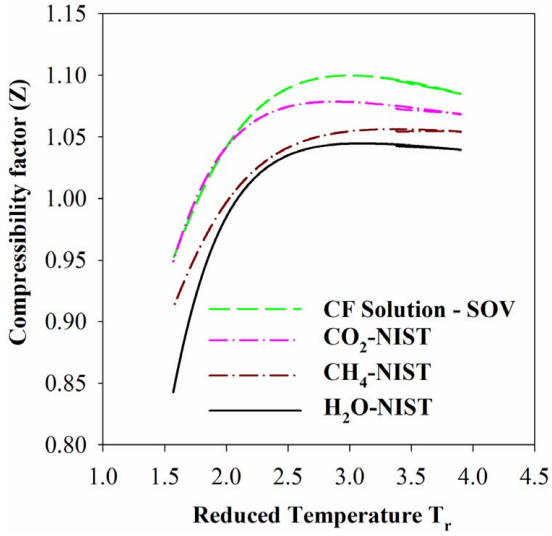

Fig. 4 Variation of the compressibility factor of various pure fluids at the P_r (from Fig. 3) and T_r in counter-flow sCO_2 flame with 96% CO_2 in the oxidizer stream

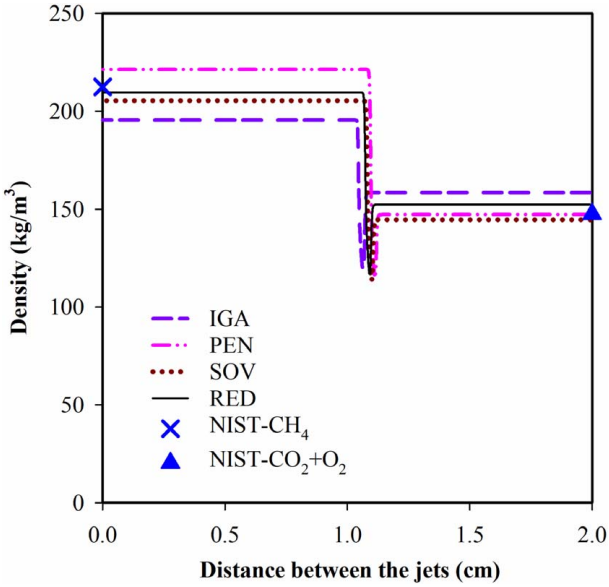

Fig. 6 Density variation in sCO_2 counter-flow flame using various EOSs with 96% CO_2 in the oxidizer stream

Further, it is important to note that density is such a quantity where its accuracy is very important in combustion modeling. A 10% error in properties like dynamic viscosity might not be significant in a turbulent combustion simulation, but a 10% error in density could result in a significant difference in kinetics, heat release rate, total enthalpy, and other important parameters. Therefore, it is very important to verify the applicability of the corresponding-state principle in the sCO_2 combustion regime and determine the possibility of obtaining accurate density predictions if the corresponding-state principle is used in simulation to account for non-ideal effects.

Figures 4 and 5 show the variation of compressibility factor of combustion mixtures in counter-flow jets with different concentrations of CO_2 present in the oxidizer stream, respectively, and shows the compressibility factor of pure CO_2, CH_4, and H_2O at the same P_r and T_r encountered in counter-flow sCO_2 flame solution. The horizontal axis in these figures represents T_r at each axial nodal point between the jets. Each T_r will have a corresponding P_r as shown in Fig. 3 (not shown in Figs. 4 and 5). The vertical axis is z. Computed z with SOV EOS are shown as "CF solution-SOV" in the legend. The compressibility factors for CO_2, CH_4, and H_2O are obtained from NIST-REFPROP [44].

A close observation of compressibility factor variation for CO_2, CH_4, and H_2O with T_r shows that there is up to 10% difference between z values (in Fig. 4). Hence, it is not easy to pick a reference fluid in order to use BWR EOS with the ECS principle. Choosing BWR constants of a random reference fluid may result in simulation inaccuracy. Secondly, SOV EOS could predict z trend the same as of NIST-REFPROP. The issue here is it is difficult to give merit to either of SOV (van der Waal types EOS) and BWR EOS–ECS approaches for accuracy because there is no data to validate. Hence, computationally easier approaches such as van der Waal type EOSs are very attractive. In the future, it is very crucial to focus on obtaining experimental data to modify van der Waal type EOSs for sCO_2 combustion applications.

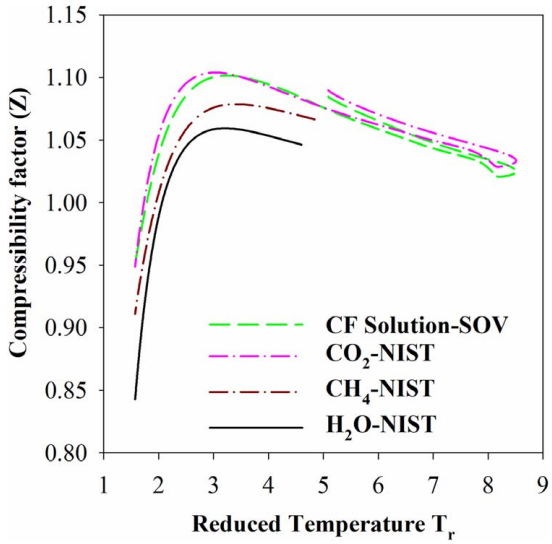

Fig. 5 Variation of the compressibility factor of various pure fluids at the P_r (from Fig. 3) and T_r in counter-flow sCO_2 flame with 35% CO_2 in the oxidizer stream

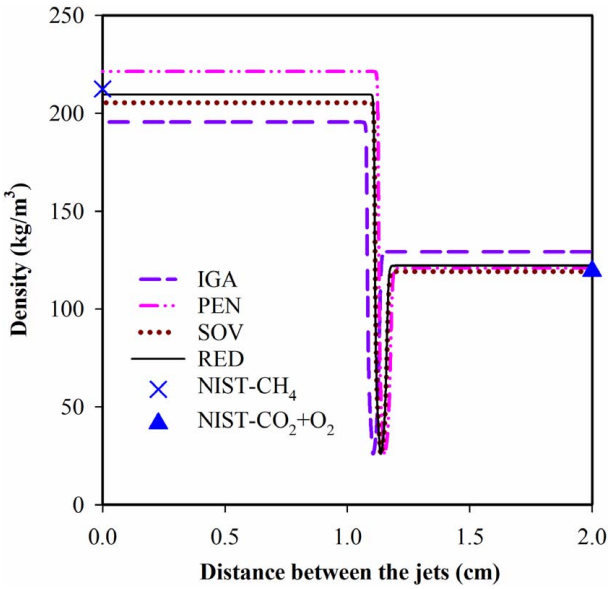

Fig. 7 Density variation in sCO_2 counter-flow flame using various EOSs with 35% CO_2 in the oxidizer stream

3.2.2 van der Waal Type Equation-of-State. As discussed in the introduction, van der Waal type EOSs are relatively simple to implement in the combustion solver and faster to solve. Also, the various parameters in the formulations of these EOSs (as shown in Table 1) are based more on physics. However, as these EOSs are empirical, adopting them to an application requires validation. There are some endeavors which are currently under progress to obtain the validating data to modify these EOSs for sCO_2 applications [18], but scanty at this moment. Therefore, in this work focus is limited to understand the applicability and effect of PEN, SOV, and RED EOSs on sCO_2 combustion.

Figures 6 and 7 display the variation of predicted density between the fuel and oxidizer streams when higher and lower concentrations of CO_2 are present in the oxidizer stream. Here, the horizontal axis represents the distance between the jets. Inlet conditions of the jets are as described in Table 2. Pure methane jet is entering at $x = 0$ cm and a mixture of CO_2 and O_2 is entering at $x = 2$ cm. As described, there is no reference data available for mixtures which can occur between these two jets. Hence, only methane and CO_2+O_2 mixture densities from NIST are shown at $x = 0$ and 2 cm, respectively.

The results indicate that, at the fuel inlet, the choice of EOS has a significant impact. Here, the difference between IGA and PEN EOSs is up to 15% (in Figs. 6 and 7). Hence, there is a possibility of significant error in the fuel mass entering the combustion reactor, if care is not taken in choosing the EOS. The impact of choice of EOS is less toward the oxidizer side. Also, toward the fuel jet, SOV and RED are closer to NIST and all real gas EOSs are closer to NIST toward the oxidizer jet. It clearly shows that IGA is not suitable for sCO_2 combustion simulation.

A general assumption is that at high temperatures, real gas also behaves like an ideal gas. But this assumption cannot be applied to non-premixed combustor simulations because fuel and oxidizer inlet jets are coming from low-temperature storage tanks and the choice of EOSs can have a significant impact. The density variation close to the flame in Figs. 6 and 7 is magnified and is shown in Figs. 8 and 9, respectively. It is interesting to see the density variation in the flame zone due to the choice of the EOS. These figures show that the choice of EOS not only affects the state but also the momentum of the jets and hence the flame structure. The lowest density point in the density profile is the highest temperature location in the flame and is slightly different between EOSs.

Also, in Figs. 8 and 9, PEN EOS estimates higher density due to which the fuel jet momentum is higher and pushes the flame more toward the oxidizer jet and it is vice versa with the IGA assumption. The SOV and RED EOS predictions are slightly distinct in Fig. 8 and overlapping in Fig. 9, which shows that when there is less CO_2 in the oxidizer stream, SOV and RED EOS are almost the same. In further sections, the reasons of this behavior are discussed.

Further, it is interesting to look at the mass fractions of CO by various EOSs. Figures 10 and 11 show the variation of CO mass fraction when higher and lower concentrations of CO_2 are present in the oxidizer stream. The presence of CO_2 increases the specific heat of the mixture and results in a lower temperature in the reaction zone, see Figs. 12 and 13. Maximum temperature with 96% CO_2 in the oxidizer stream is ~1250 K, whereas with 35% CO_2 in the oxidizer stream it is 3500 K. Chemical kinetic pathways are significantly different in high-temperature and low-temperature methane combustion [45]. Therefore, the maximum yield of CO is different.

The higher concentration of CO in Case-2 (as shown in Fig. 11) is the reason why SOV and RED are behaving the same when there is lower CO_2 concentration in the oxidizer. As shown in Table 1, the only additional term in SOV compared to RED is the term *l* which is

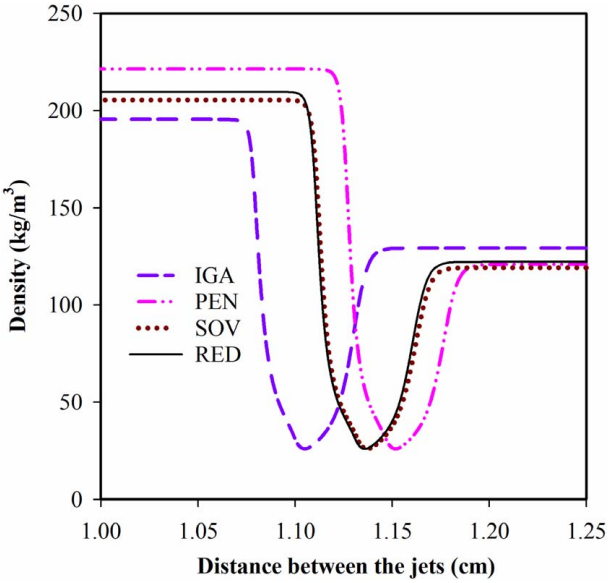

Fig. 9 Magnified view of density variation in sCO_2 counter-flow flame using various EOSs with 35% CO_2 in the oxidizer stream

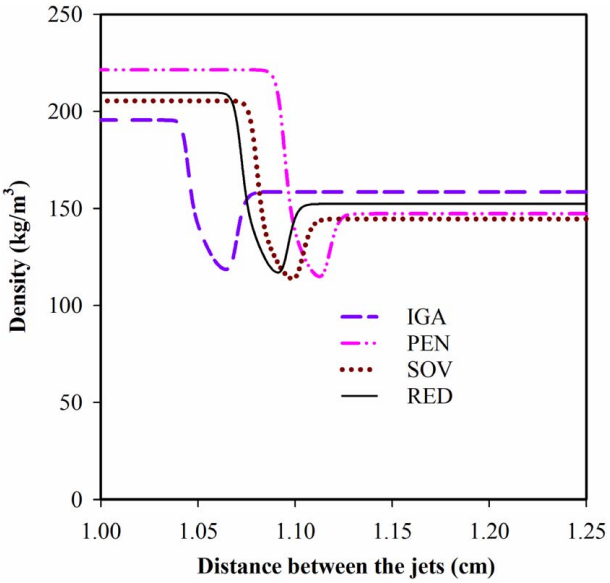

Fig. 8 Magnified view of density variation in sCO_2 counter-flow flame using various EOSs with 96% CO_2 in the oxidizer stream

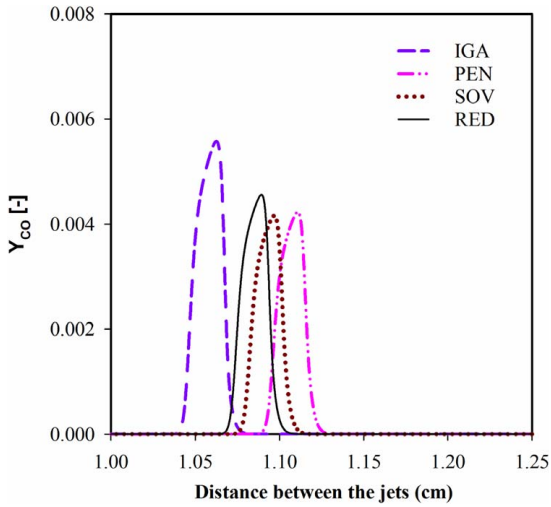

Fig. 10 Variation of mass fraction of CO in sCO_2 counter-flow flame using various EOSs with 96% CO_2 in the oxidizer stream

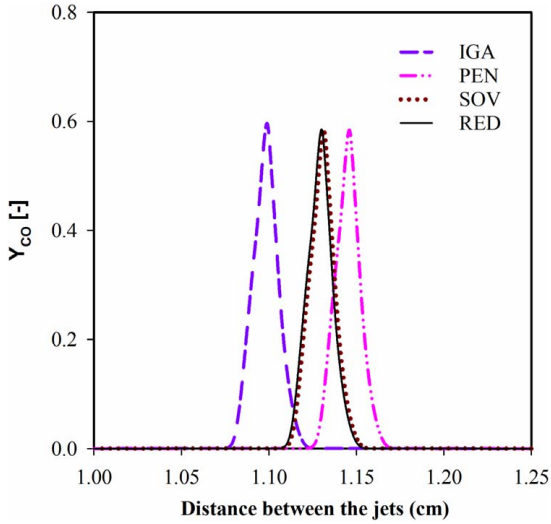

Fig. 11 Variation of mass fraction of CO in sCO_2 counter-flow flame using various EOSs with 35% CO_2 in the oxidizer stream

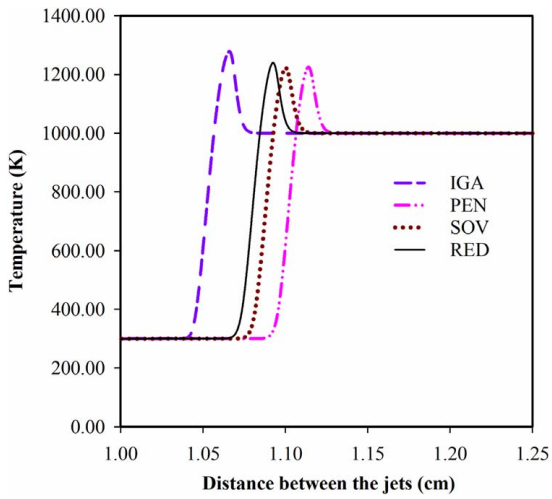

Fig. 12 Variation of temperature in sCO_2 counter-flow flame using various EOSs with 96% CO_2 in the oxidizer stream

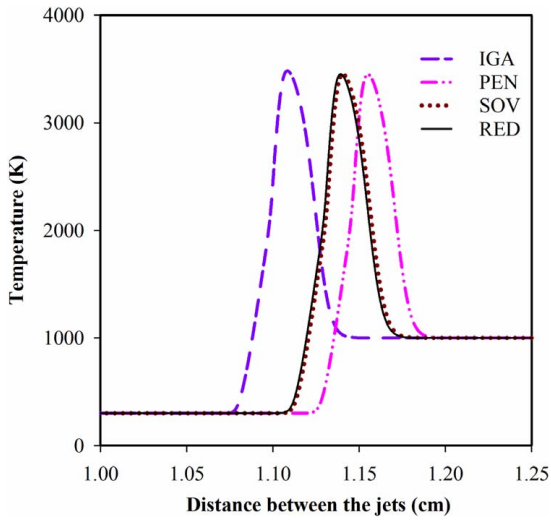

Fig. 13 Variation of temperature in sCO_2 counter-flow flame using various EOSs with 35% CO_2 in the oxidizer stream

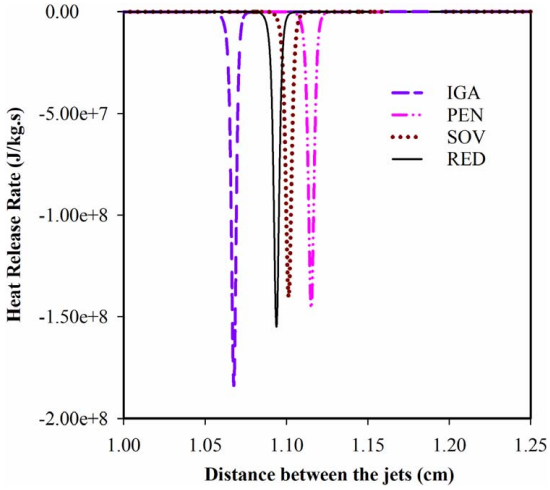

Fig. 14 Variation of heat release rate in sCO_2 counter-flow flame using various EOSs with 96% CO_2 in the oxidizer stream

a function of acentric factor (ω) and reduced temperature (T_r). The ω of CO is very small and the combined effect of this with the values of T_r brings the l factor close to unity. Hence, SOV and RED behave similarly.

Another very important parameter that needs attention in a combustion simulation is the heat release rate. Generally, chemical kinetics influence this parameter. Whereas the following result shows that the choice of EOSs also affects this parameter. This parameter is responsible for thermo acoustic oscillations in the combustion chamber, hence understanding the effect of EOSs on this quantity is very important. This quantity is estimated as shown in Eq. (6)

$$\text{Heat release rate} = \sum_{i}^{kk} \dot{\omega}_i h_{fi}/\rho \tag{6}$$

Here, $\dot{\omega}$ is the molar production rate of species $'i'$ (mol/m^{3}s), h_f is the heat of formation in molar units (J/mol), kk is the number of species, and ρ is the density (kg/m^3).

Figures 14 and 15 indicate the heat release rate when higher and lower concentrations of CO_2 are present in the oxidizer stream. The results show that the choice of EOS influences the magnitude of peak heat release rate and the difference between peak value of IGA and SOV is as much as 40%. Here, negative values of heat

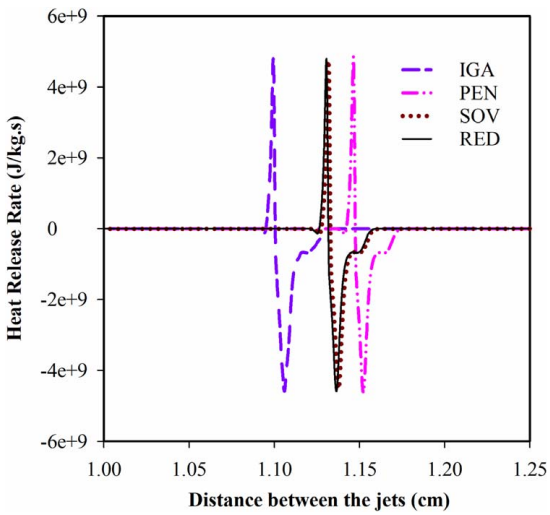

Fig. 15 Variation of heat release rate in sCO_2 counter-flow flame using various EOSs with 35% CO_2 in the oxidizer stream

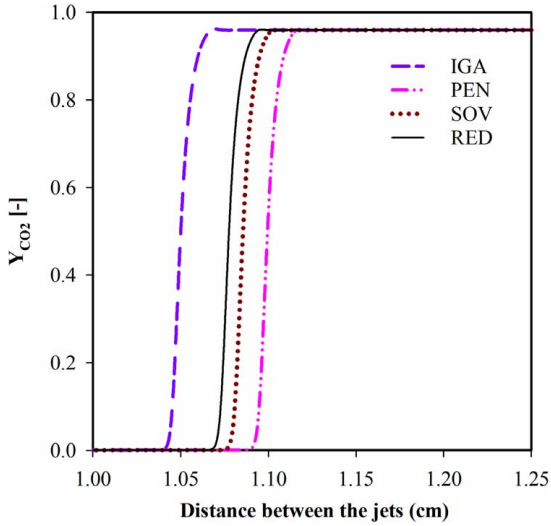

Fig. 16 Variation of Y_{CO_2} in sCO_2 counter-flow flame using various EOSs with 96% CO_2 in the oxidizer stream

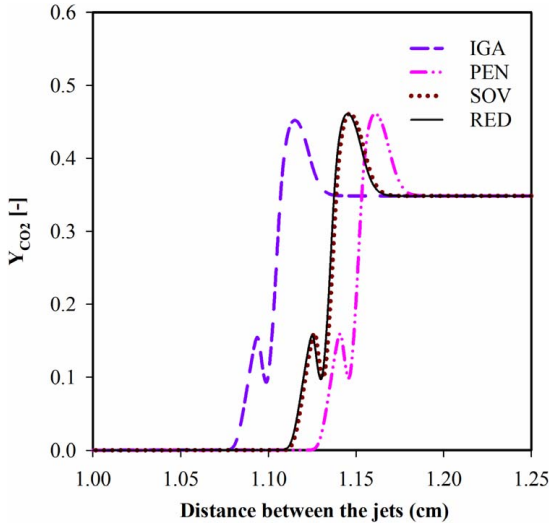

Fig. 17 Variation of Y_{CO_2} in sCO_2 counter-flow flame using various EOSs with 35% CO_2 in the oxidizer stream

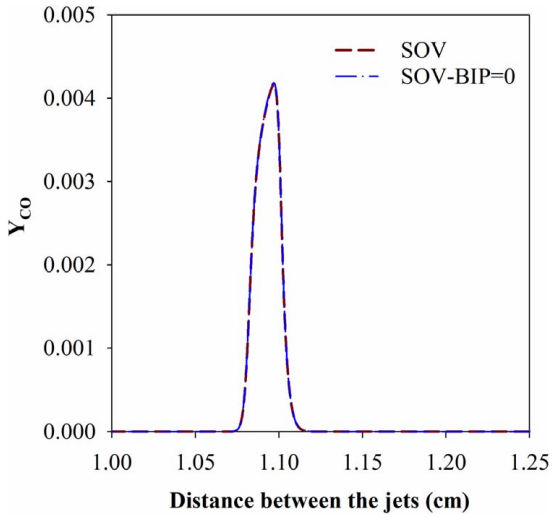

Fig. 18 Variation of Y_{CO} in sCO_2 counter-flow flame using SOV EOS by accounting proper k_{ij} and $k_{ij}=0$ with 96% CO_2 in the oxidizer stream

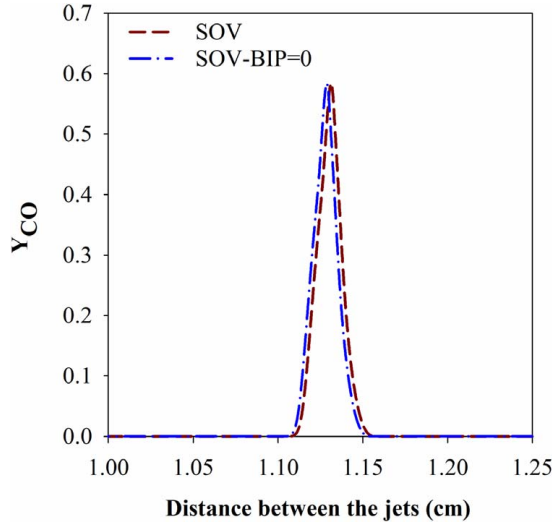

Fig. 19 Variation of Y_{CO} in sCO_2 counter-flow flame using SOV EOS by accounting proper k_{ij} and $k_{ij}=0$ with 35% CO_2 in the oxidizer stream

release rate illustrate that there is heat release from the reaction and positive value illustrates that there is heat absorption. Figure 15, i.e., Case 2, has both heat release and heat absorption during combustion. It is due to the dissociation of CO_2 as follows: Figs. 16 and 17 demonstrate the mass fractions of CO_2 between the counter-flow jets when higher and lower concentrations of CO_2 are present in the oxidizer stream. In Fig. 17, a small peak can be observed toward the fuel jet where CO_2 is dissociating and absorbing the heat.

3.3 Binary Interaction Parameter. A binary interaction parameter k_{ij} (as in Eq. (2)) accounts for deviations from ideal mixing rules as shown in Eq. (2). These parameters, in general, cannot be predicted in advance from theory, but they can be regressed from experimental measurements on the binary pairs that form the systems of interest [46]. Importantly, these parameters can have a dramatic effect on the predicted properties if the constituents have relatively a large difference in molecular weights. Obtaining these parameters for all the species involved in combustion is very difficult, however, some of this data can be obtained from the sources [37,40]. It is also a usual practice to assume binary interaction parameter as zero when appropriate information about k_{ij} is unavailable.

A numerical experiment is performed here to understand the influence of accounting for k_{ij} from the available literature and assuming $k_{ij}=0$ in sCO_2 combustion simulations. Figures 18 and 19 compare CO mass fraction between the jets by two different k_{ij} assumptions when higher and lower concentrations of CO_2 are present in the oxidizer stream. Here, brown-dash lines indicate that appropriate k_{ij} are accounted in the simulation and blue-dash-dot lines indicate that all binary interaction parameters are assumed zero. Here, dash lines indicate that appropriate k_{ij} are accounted in the simulation and dash-dot lines indicate that all binary interaction parameters are assumed zero.

Figure 18 shows that there is no effect of assuming $k_{ij}=0$ and Fig. 19 shows that there is very small difference. It is because, in Case 2, intermediate radicals are present in higher concentration. Hence, interaction parameter is important, but under current testing conditions they are not significant.

4 Conclusions

A counter-flow sCO_2 combustion simulation is performed by using state-of-the-art real gas models to understand the effect and applicability of virial and van der Waal type EOSs. Here, viscosity

and thermal conductivity are modeled by Lucas, and Steil and Thodos model, respectively. sCO_2 kinetics are considered from the UCF 1.1 mechanism. The result shows:

(1) The choice of EOS does not influence the range and the profile of reduced properties in the sCO2 combustion.
(2) BWR EOS in conjunction with ECS principle cannot be justified as accurate for combustion mixtures, because corresponding-state principle is not accurate for density estimation of mixtures.
(3) The van der Waal type EOSs can equally predict the compressibility factor as par with BWR EOS. No experimental data for the densities of sCO2 mixtures are available to estimate the performance of the van der Waal type EOSs.
(4) Non-ideal effects are significant on the fuel jet. Approximately 12% difference in density is observed between PEN and IGA. SOV and RED are closer to the reference fuel density.
(5) Choice of EOS significantly influences the momentum of jets, flame structure, heat release rate, etc.
(6) When there are lower concentrations of CO_2 present in the oxidizer jet, SOV and RED EOS behave in the same way. It is because under these conditions significant CO mass fraction is generated. Due to the low value of the acentric factor of CO, predictions of SOV and RED EOS are necessarily the same.
(7) Binary interaction parameters are not very significant in natural gas sCO_2 combustion simulations; hence can be assumed safely as zero. The influence of binary interaction parameters on complex hydrocarbon fuels is yet to be understood.

Acknowledgment

This material is based upon work supported by the Department of Energy under Award Number DE-FE0025260. This material is also based upon work partially supported by the Army Small Business Technology Transfer (STTR) Program Office under Contract No. W31P4Q-16-C-0119, Dr. Kevin Kennedy COR. Any opinions, findings, and conclusions or recommendations expressed in this material are those of the authors and do not necessarily reflect the views of the Army STTR Program Office.

This report was prepared as an account of work sponsored by an agency of the United States Government. Neither the United States Government nor any agency thereof, nor any of their employees, makes any warranty, express or implied, or assumes any legal liability or responsibility for the accuracy, completeness, or usefulness of any information, apparatus, product, or process disclosed, or represents that its use would not infringe privately owned rights. Reference herein to any specific commercial product, process, or service by trade name, trademark, manufacturer, or otherwise does not necessarily constitute or imply its endorsement, recommendation, or favoring by the United States Government or any agency thereof. The views and opinions of authors expressed herein do not necessarily state or reflect those of the United States Government or any agency thereof.

Conflict of Interest

There are no conflicts of interest.

References

[1] Brun, K., Friedman, P., and Dennis, R., 2017, *Fundamentals and Applications of Supercritical Carbon Dioxide (sCO_2) Based Power Cycles*, Woodhead Publishing, Cambridge, MA.
[2] Dostal, V., Driscoll, M. J., and Hejzlar, P., 2004, "A Supercritical Carbon Dioxide Cycle for Next Generation Nuclear Reactors," Massachusetts Institute of Technology, Department of Nuclear Engineering, Cambridge, MA.
[3] Allam, R., Fetvedt, J., Forrest, B., and Freed, D., "The Oxy-Fuel, Supercritical CO_2 Allam Cycle: New Cycle Developments to Produce Even Lower-Cost Electricity From Fossil Fuels Without Atmospheric Emissions," ASME Turbo Expo 2014: Turbine Technical Conference and Exposition, American Society of Mechanical Engineers, New York, V03BT36A016.
[4] NetPower, 2018, "Natural Gas, Syngas, or Oil Allam Cycle CCS Power Plant."
[5] Masunov, A. E., Wait, E., and Vasu, S. S., 2017, "Quantum Chemical Study of CH_3+ O_2 Combustion Reaction System: Catalytic Effects of Additional CO_2 Molecule," J. Phys. Chem. A, **121**(30), pp. 5681–5689.
[6] Masunov, A. E., Wait, E. E., Atlanov, A. A., and Vasu, S. S., 2017, "Quantum Chemical Study of Supercritical Carbon Dioxide Effects on Combustion Kinetics," J. Phys. Chem. A, **121**(19), pp. 3728–3735.
[7] Masunov, A. E., Wait, E. E., and Vasu, S. S., 2018, "Catalytic Effect of Carbon Dioxide on Reaction $OH + CO \rightarrow H + CO_2$ in Supercritical Environment: Master Equation Study," J. Phys. Chem. A, **122**(31), pp. 6355–6359.
[8] Neupane, S., Rahman, R. K., Masunov, A. E., and Vasu, S. S., 2019, "Theoretical Calculation of Reaction Rates and Combustion Kinetic Modeling Study of Triethyl Phosphate (TEP)," J. Phys. Chem. A, **123**(22), pp. 4764–4775.
[9] Pryor, O., Barak, S., Koroglu, B., Ninnemann, E., and Vasu, S. S., 2017, "Measurements and Interpretation of Shock Tube Ignition Delay Times in Highly CO2 Diluted Mixtures Using Multiple Diagnostics," Combust. Flame, **180**, pp. 63–76.
[10] Shao, J., Choudhary, R., Davidson, D. F., Hanson, R. K., Barak, S., and Vasu, S., 2019, "Ignition Delay Times of Methane and Hydrogen Highly Diluted in Carbon Dioxide at High Pressures up to 300 atm," Proc. Combust. Inst., **37**(4), pp. 4555–4562.
[11] Rahman, R. K., Barak, S., (Raghu) Manikantachari, K. R. V., Ninnemann, E., Hosangadi, A., Zambon, A., and Vasu, S. S., 2020, "Probing the Effects of NOx and SOx Impurities on Oxy-Fuel Combustion in Supercritical CO_2: Shock Tube Experiments and Chemical Kinetic Modeling," ASME J. Energy Resour. Technol., **142**(12), p. 122302.
[12] Laich, A. R., Baker, J., Ninnemann, E., Sigler, C., Naumann, C., Braun-Unkhoff, M., and Vasu, S. S., 2020, "Effects of High Fuel Loading and CO_2 Dilution on Oxy-Methane Ignition Inside a Shock Tube at High Pressure," ASME J. Energy Resour. Technol., **142**(10), p. 102103.
[13] Barak, S., Pryor, O., Ninnemann, E., Neupane, S., Vasu, S., Lu, X., and Forrest, B., 2020, "Ignition Delay Times of Oxy-Syngas and Oxy-Methane in Supercritical CO_2 Mixtures for Direct-Fired Cycles," ASME J. Eng. Gas Turbines Power, **142**(2), p. 021014.
[14] Karimi, M., Ochs, B., Liu, Z., Ranjan, D., and Sun, W., 2019, "Measurement of Methane Autoignition Delays in Carbon Dioxide and Argon Diluents at High Pressure Conditions," Combust. Flame, **204**, pp. 304–319.
[15] Manikantachari, K., Vesely, L., Martin, S., Bobren-Diaz, J. O., and Vasu, S., 2018, "Reduced Chemical Kinetic Mechanisms for Oxy/Methane Supercritical CO_2 Combustor Simulations," ASME J. Energy Resour. Technol., **140**(9), p. 092202.
[16] Kancherla, R. V. M., Martin, S. M., Bobren, J. O., and Vasu, S., 2017, "The Influence of Elevated Pressures on the Methane Combustion in N_2 and CO_2 Dilutions," 53rd AIAA/SAE/ASEE Joint Propulsion Conference, Atlanta, GA, July 10–12.
[17] Manikantachari, K. R. V., Martin, S., Rahman, R. K., Velez, C., and Vasu, S., "A General Study of Counterflow Diffusion Flames for Supercritical CO_2 Mixtures," ASME Turbo Expo 2019: Turbomachinery Technical Conference and Exposition, Phoenix, AZ, June 17–21, p.V04AT04A021.
[18] Park, S., Urso, J., (Raghu) Manikantachari, K. R. V., Hosangadi, A., Zambon, A., and Vasu, S. S., 2020, "Measurements of Density and Sound Speed in Mixtures Relevant to Supercritical CO_2 Cycles," ASME J. Energy Resour. Technol **142**(10), p. 102105.
[19] Manikantachari, K. R. V., Martin, S., Bobren-Diaz, J. O., and Vasu, S., 2017, "Thermal and Transport Properties for the Simulation of Direct-Fired sCO_2 Combustor," ASME J. Eng. Gas Turbines Power, **139**(12), p. 121505.
[20] Park, S., Kim, G., Terracciano, A. C., and Vasu, S., 2020, "High-Pressure Ignition and Flame Propagation Measurements of CO_2 Diluted Natural Gas/Oxidizer Mixtures for Advanced Rocket and Gas Turbine Combustors," AIAA Scitech 2020 Forum, Orlando, FL, Jan. 6–10.
[21] Delimont, J., Andrews, N., and Chordia, L., "Computational Modeling of a 1MW Scale Combustor for a Direct Fired sCO_2 Power Cycle," ASME Turbo Expo 2018: Turbomachinery Technical Conference and Exposition, V009T38A025.
[22] Manikantachari, K. R. V., Martin, S., Rahman, R. K., Velez, C., and Vasu, S., 2019, "A General Study of Counterflow Diffusion Flames for Supercritical CO2 Combustion," ASME J. Eng. Gas Turbines Power, **141**(12), p. 121020.
[23] Vesely, L., Dostal, V., Kapat, J., Vasu, S., and Martin, S., "Techno-Economic Evaluation of the Effect of Impurities on the Performance of Supercritical CO2 Cycles," ASME Turbo Expo 2019: Turbomachinery Technical Conference and Exposition, V009T38A014.
[24] Vesely, L., Manikantachari, K. R. V., Vasu, S., Kapat, J., Dostal, V., and Martin, S., 2018, "Effect of Impurities on Compressor and Cooler in Supercritical CO_2 Cycles," ASME J. Energy Resour. Technol., **141**(1), p. 012003.
[25] Manikantachari, K. R. V., Martin, S., Vesely, L., Bobren-Diaz, J. O., Vasu, S., and Kapat, J., "A Strategy of Reactant Mixing in Methane Direct-Fired sCO_2 Combustors," ASME Turbo Expo 2018: Turbomachinery Technical Conference and Exposition, V009T38A008.
[26] Manikantachari, K. R. V., Martin, S., Vesely, L., Bobren-Diaz, J. O., Vasu, S., and Kapat, J., "A Strategy of Mixture Preparation for Methane Direct-Fired sCO_2 Combustors," ASME Turbo Expo 2018: Turbomachinery Technical Conference and Exposition, V009T38A009.
[27] Strakey, P. A., 2019, "Oxy-Combustion Modeling for Direct-Fired Supercritical CO_2 Power Cycles," ASME J. Energy Resour. Technol., **141**(7), p. 070706.
[28] Khadse, A., Blanchette, L., Kapat, J., Vasu, S., Hossain, J., and Donazzolo, A., 2018, "Optimization of Supercritical CO_2 Brayton Cycle for Simple Cycle Gas

Turbines Exhaust Heat Recovery Using Genetic Algorithm," ASME J. Energy Resour. Technol., **140**(7), p. 071601.
[29] Liang, W., Li, W., and Law, C. K., 2019, "Laminar Flame Propagation in Supercritical Hydrogen/air and Methane/air Mixtures," Proc. Combust. Inst., **37**(2), pp. 1733–1739.
[30] Wang, X., Huo, H., and Yang, V., 2015, "Counterflow Diffusion Flames of Oxygen and N-Alkane Hydrocarbons (CH_4-$C_{16}H_{34}$) at Subcritical and Supercritical Conditions," Combust. Sci. Technol., **187**(1–2), pp. 60–82.
[31] Huo, H., Wang, X., and Yang, V., 2014, "A General Study of Counterflow Diffusion Flames at Subcritical and Supercritical Conditions: Oxygen/Hydrogen Mixtures," Combust. Flame, **161**(12), pp. 3040–3050.
[32] Sengers, J. V., Kayser, R., Peters, C., and White, H., 2000, *Equations of State for Fluids and Fluid Mixtures*, Elsevier, New York.
[33] Valderrama, J. O., 2003, "The State of the Cubic Equations of State," Ind. Eng. Chem. Res., **42**(8), pp. 1603–1618.
[34] Yang, V., 2000, "Modeling of Supercritical Vaporization, Mixing, and Combustion Processes in Liquid-Fueled Propulsion Systems," Proc. Combust. Inst., **28**(1), pp. 925–942.
[35] Patel, N. C., 1980, "The Calculation of Thermodynamic Properties and Phase Equilibria Using a new Cubic Equation of State," © Navin C. Patel.
[36] Stiel, L. I., and Thodos, G., 1964, "The Thermal Conductivity of Nonpolar Substances in the Dense Gaseous and Liquid Regions," AIChE J., **10**(1), pp. 26–30.
[37] Poling, B. E., Prausnitz, J. M., and O'connell, J. P., 2001, *The Properties of Gases and Liquids*, McGraw-Hill, New York.
[38] Lucas, K., 1981, "Die Druckabhängigkeit der Viskosität von Flüssigkeiten—Eine Einfache Abschätzung," Chem. Ing. Tech., **53**(12), pp. 959–960.
[39] Wang, C.-H., Masunov, A. M. E., Allison, T. C., Chang, S., Lim, C., Jin, Y., and Vasu, S. S., 2019, "Molecular Dynamics of Combustion Reactions in Supercritical Carbon Dioxide. 6. Computational Kinetics of Reactions Between Hydrogen Atom and Oxygen Molecule $H + O_2 \rightleftharpoons HO + O$ and $H + O_2 \rightleftharpoons HO_2$," J. Phys. Chem. A, **123**(50), pp. 10772–10781.
[40] Schmitt, R. G., Butler, P. B., and French, N. B., 1994, *Chemkin Real Gas: A Fortran Package for Analysis of Thermodynamic Properties and Chemical Kinetics in Nonideal Systems*, University of Iowa, Iowa City.
[41] Lutz, A. E., Kee, R. J., Grcar, J. F., and Rupley, F. M., 1997, *OPPDIF: A Fortran Program for Computing Opposed-Flow Diffusion Flames*, Sandia National Labs., Livermore, CA.
[42] Oefelein, J. C., 2006, "Mixing and Combustion of Cryogenic Oxygen-Hydrogen Shear-Coaxial Jet Flames at Supercritical Pressure," Combust. Sci. Technol., **178**(1–3), pp. 229–252.
[43] Cengel, Y. A., and Boles, M. A., 2007, *Thermodynamics: An Engineering Approach*, 6th ed., The McGraw-Hill Companies, Inc., New York.
[44] Lemmon, E. W., Huber, M. L., and McLinden, M. O., 2002, "NIST Reference Fluid Thermodynamic and Transport Properties–REFPROP," NIST Standard Reference Database, 23, p. v7.
[45] Turns, S. R., 2012, *An Introduction to Combustion: Concepts and Applications*, McGraw-Hill, New York.
[46] Abudour, A. M., Mohammad, S. A., Robinson R. L., Jr., and Gasem, K. A. M., 2014, "Generalized Binary Interaction Parameters for the Peng–Robinson Equation of State," Fluid Phase Equilib., **383**, pp. 156–173.